Isomer Separation

DOI: 10.1002/ange.201408981

C_{60}-Mediated Molecular Shape Sorting: Separation and Purification of Geometrical Isomers**

*Moumita Rana, R. Bharathanatha Reddy, Bibhuti Bhusan Rath, and Ujjal K. Gautam**

Abstract: *A supramolecular crystallization-based approach has been developed for the shape-dependent separation of geometrical isomers under near-ambient conditions. Difficulties to separate such isomers arise because of their very similar physical properties. The present approach relies on the ability of C_{60} to preferentially form solvate crystals with molecules of a specific geometry. Subsequently, these molecules are released upon mild heating to regenerate pure C_{60}. By taking isomers of xylene and trimethylbenzene (TMB) as examples, we show that one of the isomers can be extracted from the rest with very high purity. To separate TMB isomers, a new C_{60}–1,3,5-TMB solvate was developed, which led to the isolation of isomer purities greater than 99.6 %. Versatility, a low operating temperature of approximately 100 °C, a separation efficiency of more than 10 weight % of C_{60} per cycle, and reagent recyclability makes this a promising molecular shape-sorting approach.*

The separation of geometrically different isomers of small organic compounds is an expensive and difficult process, constituting a major industrial challenge. Such difficulties arise as a result of the similar physical properties of isomers, such as molecular weight, phase transition temperatures, and dielectric constants.[1] Extensive investigations on this topic has led to the discovery of several separation approaches, such as chromatographic techniques using extended porous solids.[2] Tuning the chemical interactions within these pores is challenging to achieve isomer separation with sufficiently high resolution.[3] Chemical complexation or crystallization is one of the oldest separation approaches, employing clathrates, calixarenes, and other complexation reagents.[4] Despite several problems associated with this method, it remains a commercially viable approach even today. Complexation occurs because of interactions between complementary functional groups and as a result, it is rather difficult to design reagents suitable for separation of multiple sets of isomers.[5] Mitra et al. recently developed an approach which, rather than relying on host–guest interactions, created molecular organic cages with geometries suitable for only certain shapes.[6] Customized cages permit design flexibility and exceptionally high separation specificity, as only complementary shapes can be uptaken by cages.

Among the industrially important compounds, isomers of xylene and trimethylbenzene (TMB) have been extensively investigated.[7] These compounds are usually extracted as two different fractions during petroleum refining. Xylenes are obtained as a mixture of *ortho* (*o*), *para* (*p*), and *meta* (*m*) isomers. Each pure isomer is an important building block for different commercial products, such as polyethylene terephthalate (PET).[7b] The TMB fraction consists of mostly 1,2,4- and 1,3,5-substituted isomers, which are used as scintillators and colorants, respectively.[7a] Separation of these isomers involves a combination of techniques including fractional distillation, complexation, and absorption in nanoscale pores. Only *o*-xylene is separated by distillation, despite the poor efficiency of the process. The separation of *para* and *meta* isomers is more difficult because of the formation of a eutectic mixture and requires complex formation with the highly toxic compound $HF–BF_3$.[8] Separation of the TMB isomers is usually carried out employing an azeotropic distillation process.[9] Chromatographic separation techniques for these compounds are typically environmentally benign, despite requiring large quantities of eluents and having poor pore-filling fractions.[10] The most promising separation method for these molecules has been shown to be enclathration, however isomer recovery usually leads to byproduct formation.[11] In this regard, Barbour and Lusi have recently shown that a single Ni-based clathrate may be used to neatly separate the xylene isomers in the vapor phase.[12]

Herein, we demonstrate that fullerene C_{60} is a versatile, efficient, and recyclable crystal-forming agent for the separation of geometrical isomers under near-ambient conditions. Fullerenes are the only soluble allotrope of carbon, enabling their simple processing for use in applications including electronic devices, energy harvesting, and in biomedical research.[13] C_{60} can form crystals with solvent molecules of an appropriate size and shape, and these crystals can exhibit fascinating properties.[14] Solvate crystals are stabilized by weak interactions between solvent and C_{60} molecules making them stable under ambient conditions.[15] Each C_{60} molecule complexes with one or two solvent molecules, leading to a very high solvent uptake ratio. Moderate heating is sufficient to induce release of the solvent molecules, leaving behind pure C_{60}. We presumed that the selective, large uptake of molecules and their simple release should make C_{60} an interesting material for shape-selective chemical separation. Taking xylene as an example, we show that: a) *m*-xylene can

[*] M. Rana,[+] R. B. Reddy,[+] B. B. Rath, Dr. U. K. Gautam
Nanomaterials and Energy Laboratory, New Chemistry Unit
Jawaharlal Nehru Centre for Advanced Scientific Research
P.O. Jakkur, Bangalore, Karnataka-560064 (India)
E-mail: ujjalgautam@gmail.com

[+] These authors contributed equally to this work.

[**] M.R. thanks CSIR (India) for a SR fellowship. U.K.G. thanks DST (India) for a Ramanujan Fellowship and the Sheikh Saqr Laboratory for generous research funding. We sincerely thank Dr. S. K. Reddy for his input with theoretical studies. We gratefully acknowledge useful discussions with Prof. S. Balasubramaniam and Prof. S. Rajaram.

Supporting information for this article is available on the WWW under http://dx.doi.org/10.1002/anie.201408981.

be isolated from a mixture of *o*- and *p*-xylene with approximately 100% purity, and the separation efficiency per unit weight is comparable to, and sometimes even better than, zeolites, MOFs, and other reagents,[3c,5,6,7c] and b) a mild, eluent-free process can be employed to release the entrapped xylene molecules by heating to 70°C. To demonstrate the versatility of this method, we further investigate C_{60} solvate formation with TMB isomers. Herein, we report a new 1,3,5-TMB–C_{60} solvate and show that its presence as an impurity in the 1,2,4-TMB can be reduced to below 0.4% even at room temperature. Notably, the removal of trace quantities of one isomeric impurity to attain a higher purity of the individual isomers is expensive and a progressively difficult process (see Table S1 in the Supporting Information).[16] Therefore, the fact that the C_{60}-mediated method is very efficient even at extremely low isomer concentrations allows us to propose it not only as separation method, but also as a potential purification method.

m-Xylene forms solvate crystals effortlessly with C_{60} under ambient conditions.[17] Two methods were adopted to prepare the crystals. The first technique employed was the liquid–liquid interfacial precipitation (LLIP) method, where a poor solvent for C_{60}, for example, isopropanol (IPA), was slowly added to a solution of C_{60} in xylene. Alternatively, the ultrasonic liquid–liquid interfacial precipitation (ULLIP) method was used, where a solution of C_{60} was added to IPA under sonication.[18] The LLIP method takes several hours to yield crystals, whereas sonication immediately induces precipitation by the ULLIP method. Both methods result in the formation of solvate crystals with identical crystal structures, although the morphology of the crystals is different (Figure S1 in the Supporting Information). Powder XRD (PXRD) patterns indicate that C_{60}–*m*-xylene solvate molecules crystallize in a hexagonally close-packed (HCP) structure with a $P6_3$ space group (Figure 1a).[19] On the other hand, precipitation of C_{60} from a solution of *o*- or *p*-xylene yielded pure C_{60} powder (Figure 1b,c). Variations in experimental conditions did not result in the formation of solvate crystals composed of *o*- or *p*-xylene. Interestingly, in addition to the PXRD patterns, field emission scanning electron microscopy (FESEM) images show that the one-dimensional rod-shaped morphology of the solvate crystals is visually distinguishable from the pure C_{60} crystals (Figure 1d–f). The *m*-xylene solvate crystals are stable under ambient conditions for months, and can release the captured solvent molecules upon heating up to 70°C (Figure 2a). The presence of only the *meta* isomer of xylene in the solvate crystal was also confirmed by FTIR spectroscopy. The xylene isomers show distinct features in the fingerprint region of the IR spectrum. The bands at 794.5 and 742.4 cm^{-1} correspond to aromatic C–H out-of-plane (OOP) bending modes of *o*- and *p*-xylene, respectively (Figure S2), whereas the same bands for *m*-xylene are detected at 769.5 and 690.4 cm^{-1}. From Figure 2b, only bands attributable to *m*-xylene and C_{60} in the FTIR spectrum of the HCP solvate are evident. A similar FTIR investigation was useful later to infer that when a mixture of xylene isomers was separated using C_{60}, only *m*-xylene was taken up to form the HCP solvate crystal.

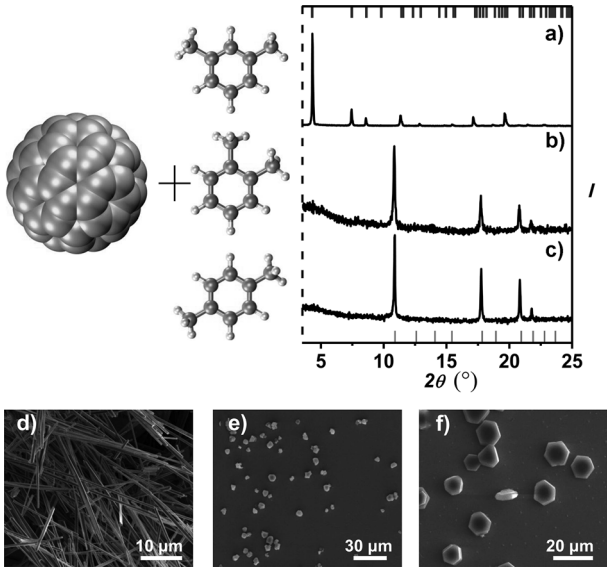

Figure 1. a–c) PXRD patterns and d–f) FESEM images of the products formed using *m*-xylene (a,d), *o*-xylene (b,e), and *p*-xylene (c,f). The vertical bars at the top and bottom (a–c) correspond to the simulated patterns of solvate HCP and pristine face-centered cubic (FCC) C_{60} crystals.

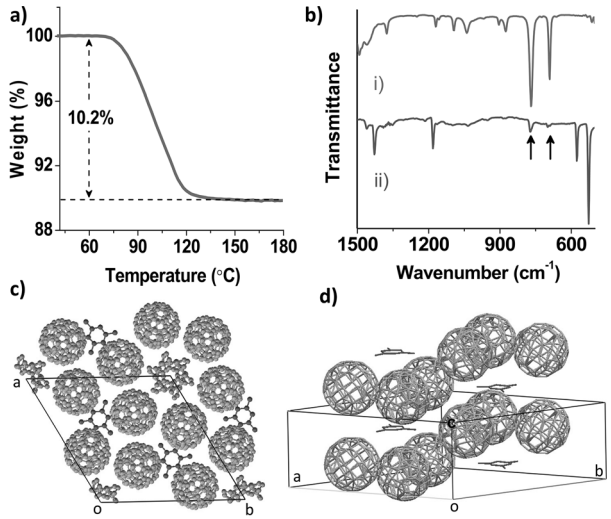

Figure 2. a) Thermogravimetric analysis of the C_{60}–*m*-xylene HCP solvate crystal showing the release of solvent molecules from the crystals, which commences at approximately 70°C. b) FTIR spectra of i) *m*-xylene and ii) its C_{60} solvate. The two marked peaks originate from *m*-xylene in the solvate crystal. Crystal structure of HCP C_{60}–*m*-xylene solvate projected c) along the *c*-axis and d) perpendicular to the *c*-axis. As a result of disorder, *m*-xylene in the C_3-symmetric site appears to be 1,3,5-TMB.

To understand such selectivity in solvate-crystal formation, we analyzed the single-crystal X-ray structure of the C_{60}–*m*-xylene solvate. Figures 2c and d depict its single-crystal structure recorded at 20 K.[19] The fullerene molecules are packed in a hexagonal lattice creating two distinct crystallographic sites for the solvent molecule with C_3 and 6_3 symmetries. In the C_3-symmetric site, the methyl substitu-

ents are disordered about the threefold axis, making *m*-xylene appear similar to 1,3,5-TMB. This allowed us to hypothesize that other suitable molecules that fit into the cavity, such as toluene[20] or 1,3,5-TMB, should also form a similar solvate structure. On the other hand, such geometric considerations rule out inclusion of *o*- or *p*-xylene, at least at 20 K. However, as a result of the high degree of rotational disorder associated with *m*-xylene at the C_3-symmetric site even at 20 K, the crystals formed at ambient temperature may not automatically completely exclude other isomers. To explore the possibility of positioning methyl groups at different positions on the benzene ring, we examined theoretically the temperature-induced deflection of the methyl groups about its mean position within the solvate crystal at 27 °C. First, the energy-minimized structure for the solvate was estimated using the experimentally obtained crystal structure (Figure S3).[21] Subsequently, the effect of temperature was examined using molecular dynamics simulations run for 5 ns at 300 K. The thermal fluctuations of the xylene methyl groups from their mean positions show a maximum deviation of $\pm 13°$ (Figure 3). This is much less than the 60° required to position an *o*- or *p*-xylene in the C_3-symmetric cavity. Therefore, doping of the *m*-xylene solvates with *ortho* or *para* isomers of xylene can be ruled out.

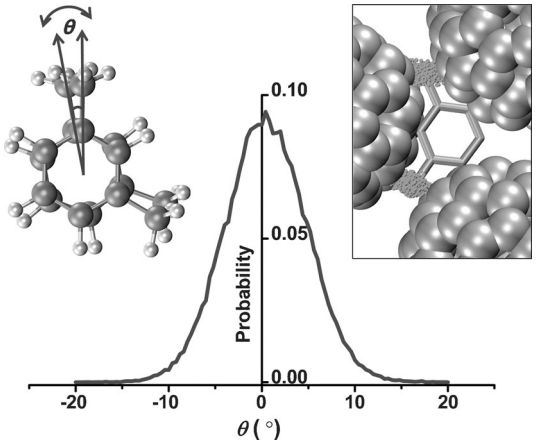

Figure 3. Thermally induced angular distribution (θ) of the methyl group of *m*-xylene within the [110] crystal plane at 300 K. Left inset: representation of θ between two xylene configurations (one being the energy minimized structure) in the crystal. Right inset: representation of the methyl group trajectories at 300 K. The trajectories of other atoms are not shown for clarity. Xylene is shown as a stick model, C_{60} is shown in space-filling representation.

We examined the precipitation rate using the LLIP and ULLIP methods at three different temperatures (5, 25, and 45 °C; Figure S4). Each experiment resulted in the formation of a HCP C_{60}–*m*-xylene solvate. However, the precipitation process is considerably faster at higher temperatures and takes only 4 hours at 45 °C as compared to 72 hours at 5 °C. We confirmed by temperature-dependent PXRD that there is no phase transition until 70 °C (Figure S5). Therefore, our hypothesis of shape selectivity should be applicable within this entire temperature range.

We performed competition experiments at 0, 5, and 27 °C by LLIP and ULLIP methods to estimate the separation efficiency of different isomers with C_{60}. Solvent mixtures of: a) *meta* and *ortho* isomers of xylene, b) *meta* and *para* isomers, and c) *ortho*, *meta*, and *para* isomers of xylene, were used to dissolve C_{60}. In each case, the solvent ratios were systematically changed and the precipitates were analyzed by XRD. It is evident that the precipitated HCP solvate crystal had taken away a fraction of *m*-xylene molecules from the solvent mixture and the remaining solvent became richer in the other isomer. We found that both methods very efficiently separate *m*-xylene, as HCP solvates form easily even when the mixture contains an extremely small quantity of the *meta* isomer. The efficiency and separation time is dependent on working temperature. The results of the competition experiments in the limiting cases, where *m*-xylene content is very low but still separable, are summarized in Table 1 (further details given in Table S2). LLIP methods at low temperatures exhibit the highest separation efficiencies. The minimum quantity of *m*-xylene which should be externally added to the *ortho* or *para* isomer to form a HCP solvate is 0.15 % and 0.5 % respectively, suggesting that the leftover xylene fractions are of very high purity (Figure S7a, b). In the case of the xylene mixture containing the three isomers, up to 0.4 % of *m*-xylene can be separated at 5 °C by the LLIP method (Figure S8). The separation efficiency is higher using the LLIP method, whereas separation using the ULLIP method is much faster. The choice of the poor solvent for C_{60} is crucial. Using methanol and ethanol, precipitation at 27 °C from a solvent mixture containing 2.5 % *m*-xylene took 16 and 30 hours, respectively, yielding pure C_{60} (Figure S11 a, b). In the case of *n*-propanol, HCP solvates formed after 4 days (Figure S11 c).

Table 1: Summary of the competition experiments using LLIP and ULLIP methods.

Method	*T* [°C]	Isomer [%][b]			Product crystal structure[a, c]
		o-xylene	*p*-xylene	*m*-xylene	
LLIP	0	99.85	0	0.15	HCP (+ FCC)
LLIP	5	0	99.6	0.4	HCP (+ FCC)
LLIP	5	49.8	49.8	0.4	HCP (+ FCC)
LLIP	27	0	97.5	2.5	HCP
ULLIP	1	99.75	0	0.25	HCP (+ FCC)
ULLIP	5	0	99	1	HCP

[a] Formation of the HCP solvate indicates separation of *m*-xylene from the solvent mixture containing different xylene isomers. [b] Percentage indicates the fraction of each isomer of xylene in the solvent mixture. [c] For some experiments, small amounts of pure face-centered cubic (FCC) C_{60} crystals form in addition to HCP solvate crystals. Total volume of the xylene mixture: 2000 μL.

The release of entrapped xylene molecules begins at 70 °C accompanied by a weight loss of 10.2 % (Figure 2 a), attributable to the loss of one *m*-xylene molecule per C_{60}. We examined the release of *m*-xylene molecules at 70 °C by monitoring changes in the crystal structure (Figure 4). The enthalpy change corresponding to the release of *m*-xylene was estimated to be -6.39 kcal mol^{-1} (Figure S12 a). The solvate

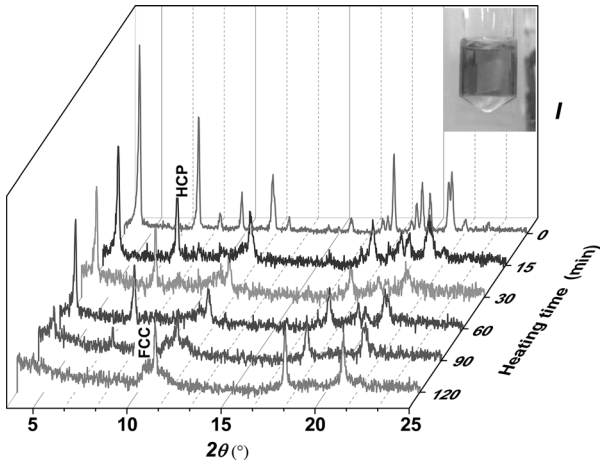

Figure 4. Time evolution of the XRD pattern of the *m*-xylene solvates at 70 °C marking the release of entrapped molecules. Inset: the complete dissolution of the recycled C_{60} in xylene.

complexes degrade over 120 minutes. This sufficiently low-temperature release ensures that the C_{60} remains pure, unpolymerized (Figure S12b,c), and ready for the next separation cycle. This 10% extraction ability, that is, one molecule per C_{60} per cycle, is comparable to other separation approaches.[1d,2b,6,12,22]

Finally, to investigate the generic nature of shape selectivity in this approach, we investigated the separation of TMB isomers. Notably, even though the HCP solvate of C_{60} with these molecules has not yet been reported,[23] we hypothesized that 1,3,5-TMB with a threefold symmetry should fit in the C_3-symmetric cavity of the HCP solvate (Figure 2c). Employing the LLIP method and using a C_{60} solution in 1,3,5-TMB and IPA as the poor solvent, we obtained rod-shaped crystals, whose PXRD pattern exactly matches with that of the HCP *m*-xylene solvate (Figure S13a). This indicates the formation of a new C_{60} solvate with 1,3,5-TMB. On the other hand, precipitation from commercially available 1,2,4-TMB (98% pure) also yielded a HCP C_{60} solvate (Figure S13b), as 1,3,5-TMB contamination far exceeds its extraction limit by C_{60}. In both cases, uptake of 1,3,5-TMB by C_{60} is established by FTIR spectra (Figure S14). We purified 1,2,4-TMB using C_{60} as described below. First, we systematically diluted 1,2,4-TMB with *o*-xylene to reduce the fraction of the 1,3,5-TMB impurity, and then employed the LLIP method. It was found that upon reaching an eightfold dilution level, no more HCP solvate formed (Figure S15). Assuming that the entire 2% impurity was 1,3,5-TMB, it reduces to 0.25% of the total solution after an eightfold dilution. 1,3,5-TMB as an impurity below this level, cannot be extracted at 27 °C. However, when 1,3,5-TMB (0.15%) was intentionally added to the eightfold-diluted aliquot (which equals a maximum impurity of 0.4%), the LLIP method yielded only HCP solvate (Figure S15d). Therefore, the estimated maximum purity of the 1,2,4-TMB obtainable from the separation of its 1,3,5-isomer at 27 °C is more than 99.6% (Figure S15), a remarkably high value even in comparison to the xylene isomers (Table 1).

In summary, our results show that C_{60} can be efficiently used for separation of geometrical isomers under near-ambient conditions. There are several potential advantages of this approach, including: a) the high purity of the extracted product, b) the use of a small amount of a second solvent, c) a good uptake capacity of approximately 11%, d) the recyclability of C_{60}, and e) a versatile method. We propose that it would be possible to extend this approach for the separation of other chemical feedstocks by designing appropriate C_{60} solvate molecules. One may also envision many future challenges. In addition to high specificity, a high recovery quantity per cycle is essential for sustainable applications. The solubility of C_{60} is usually not very high and so suitable chemical modifications might be helpful.[24] We have recently inferred that excess solvate in contact with its solution may maintain dynamic equilibrium of continuous dissolution and reprecipitation,[20] suggesting that an excess of solid C_{60} in contact with a chemical feedstock may spontaneously convert into a solvate. Investigations on the possibility of isomer separation beyond the C_{60} solubility limits are currently ongoing. Preliminary results show that the current method can be extended to separate other isomers, structural analogues, aromatic-aliphatic compounds and even ternary mixtures (Table S3, Figures S16–S23). We believe that this method is an interesting addition to the many potential applications of fullerenes and should stimulate further investigations on solvates for molecular separation.

Received: September 10, 2014
Published online: October 5, 2014

Keywords: crystal growth · fullerenes · shape sorting · xylene separation

[1] a) E. D. Bloch, W. L. Queen, R. Krishna, J. M. Zadrozny, C. M. Brown, J. R. Long, *Science* **2012**, *335*, 1606 – 1610; b) A. Chauvel, G. Lefebvre, *Petrochemical Processes*, Editions OPHRYS, Paris, **1989**; c) R. M. Lima, I. E. Grossmann, *AIChE J.* **2009**, *55*, 354 – 373; d) C. J. King, *Separation Processes*, 2ednd edCourier Dover Publications, Mineola, NY, **2013**.

[2] a) S. Kulprathipanja, J. Wiley, *Zeolites in Industrial Separation and Catalysis*, Wiley Online Library, Hoboken, **2010**; b) J.-R. Li, R. J. Kuppler, H.-C. Zhou, *Chem. Soc. Rev.* **2009**, *38*, 1477 – 1504; c) T. C. T. Pham, T. H. Nguyen, K. B. Yoon, *Angew. Chem. Int. Ed.* **2013**, *52*, 8693 – 8698; *Angew. Chem.* **2013**, *125*, 8855 – 8860; d) G.-q. Guo, Y.-c. Long, *Sep. Purif. Technol.* **2001**, *24*, 507 – 518.

[3] a) L. Alaerts, M. Maes, L. Giebeler, P. A. Jacobs, J. A. Martens, J. F. M. Denayer, C. E. A. Kirschhock, D. E. De Vos, *J. Am. Chem. Soc.* **2008**, *130*, 14170 – 14178; b) Z.-Y. Gu, X.-P. Yan, *Angew. Chem. Int. Ed.* **2010**, *49*, 1477 – 1480; *Angew. Chem.* **2010**, *122*, 1519 – 1522; c) L. Alaerts, C. E. A. Kirschhock, M. Maes, M. A. van der Veen, V. Finsy, A. Depla, J. A. Martens, G. V. Baron, P. A. Jacobs, J. F. M. Denayer, D. E. De Vos, *Angew. Chem. Int. Ed.* **2007**, *46*, 4293 – 4297; *Angew. Chem.* **2007**, *119*, 4371 – 4375; d) V. Finsy, H. Verelst, L. Alaerts, D. De Vos, P. A. Jacobs, G. V. Baron, J. F. M. Denayer, *J. Am. Chem. Soc.* **2008**, *130*, 7110 – 7118.

[4] a) H. Takahagi, S. Fujibe, N. Iwasawa, *Chem. Eur. J.* **2009**, *15*, 13327 – 13330; b) H. R. Allcock, *Acc. Chem. Res.* **1978**, *11*, 81 – 87; c) J. Xing, C.-Y. Wu, T. Li, Z.-L. Zhong, Y.-Y. Chen, *Anal. Sci.* **1999**, *15*, 785 – 790.

[5] R. El Osta, A. Carlin-Sinclair, N. Guillou, R. I. Walton, F. Vermoortele, M. Maes, D. de Vos, F. Millange, *Chem. Mater.* **2012**, *24*, 2781 – 2791.

[6] T. Mitra, K. E. Jelfs, M. Schmidtmann, A. Ahmed, S. Y. Chong, D. J. Adams, A. I. Cooper, *Nat. Chem.* **2013**, *5*, 276 – 281.
[7] a) A. M. Landis, J. W. Priegnitz, US Patent No. 4,270,013, **1981**; b) J. Fabri, U. Graeser, T. A. Simo, *Ullmann's Encyclopedia of Industrial Chemistry*, Wiley-VCH, Weinheim, **2000**; c) S. J. Lue, T.-h. Liaw, *Desalination* **2006**, *193*, 137 – 143.
[8] C. J. Egan, R. V. Luthy, *Ind. Eng. Chem.* **1955**, *47*, 250 – 253.
[9] L. Berg, U. S. Patent 6,136,155, **2000**.
[10] M. O. Daramola, A. J. Burger, M. Pera-Titus, A. Giroir-Fendler, S. Miachon, J. A. Dalmon, L. Lorenzen, *Asia-Pac. J. Chem. Eng.* **2010**, *5*, 815 – 837.
[11] J. Lipkowski, D. D. MacNicol, F. Toda, R. Bishop, *Comprehensive Supramolecular Chemistry*, Pergamon, Exeter, **1996**, *6*, 691 – 714.
[12] M. Lusi, L. J. Barbour, *Angew. Chem. Int. Ed.* **2012**, *51*, 3928 – 3931; *Angew. Chem.* **2012**, *124*, 3994 – 3997.
[13] a) L. K. Shrestha, Q. Ji, T. Mori, K. i. Miyazawa, Y. Yamauchi, J. P. Hill, K. Ariga, *Chem. Asian J.* **2013**, *8*, 1662 – 1679; b) X. Zhang, S. Mizukami, T. Kubota, Q. Ma, M. Oogane, H. Naganuma, Y. Ando, T. Miyazaki, *Nat. Commun.* **2013**, *4*, 1392; c) H. Li, B. C. K. Tee, J. J. Cha, Y. Cui, J. W. Chung, S. Y. Lee, Z. Bao, *J. Am. Chem. Soc.* **2012**, *134*, 2760 – 2765; d) C. Evangeli, K. Gillemot, E. Leary, M. T. González, G. Rubio-Bollinger, C. J. Lambert, N. Agraï, *Nano Lett.* **2013**, *13*, 2141 – 2145; e) S. H. Friedman, D. L. DeCamp, R. P. Sijbesma, G. Srdanov, F. Wudl, G. L. Kenyon, *J. Am. Chem. Soc.* **1993**, *115*, 6506 – 6509.
[14] a) M. Sathish, K. Miyazawa, *J. Am. Chem. Soc.* **2007**, *129*, 13816 – 13817; b) L. Wang, B. Liu, S. Yu, M. Yao, D. Liu, Y. Hou, T. Cui, G. Zou, B. Sundqvist, H. You, D. Zhang, D. Ma, *Chem. Mater.* **2006**, *18*, 4190 – 4194; c) L. K. Shrestha, Y. Yamauchi, J. P. Hill, K. Miyazawa, K. Ariga, *J. Am. Chem. Soc.* **2013**, *135*, 586 – 589.
[15] H. Suezawa, T. Yoshida, S. Ishihara, Y. Umezawa, M. Nishio, *CrystEngComm* **2003**, *5*, 514 – 518.
[16] L.-D. Shiau, C.-C. Wen, B.-S. Lin, *Ind. Eng. Chem. Res.* **2005**, *44*, 2258 – 2265.
[17] L. Wang, B. Liu, D. Liu, M. Yao, Y. Hou, S. Yu, T. Cui, D. Li, G. Zou, A. Iwasiewicz, *Adv. Mater.* **2006**, *18*, 1883 – 1888.
[18] K. Miyazawa, Y. Kuwasaki, A. Obayashi, M. Kuwabara, *J. Mater. Res.* **2002**, *17*, 83 – 88.
[19] M. Ramm, P. Luger, D. Zobel, W. Duczek, J. C. A. Boeyens, *Cryst. Res. Technol.* **1996**, *31*, 43 – 53.
[20] M. Rana, R. R. Bharathanatha, U. K. Gautam, *Carbon* **2014**, *74*, 44 – 53.
[21] a) W. L. Jorgensen, T. B. Nguyen, *J. Comput. Chem.* **1993**, *14*, 195 – 205; b) S. Plimpton, *J. Comput. Phys.* **1995**, *117*, 1 – 19; c) B. Rousseau, J. Petravic, *J. Phys. Chem. B* **2002**, *106*, 13010 – 13017.
[22] Z.-Y. Gu, D.-Q. Jiang, H.-F. Wang, X.-Y. Cui, X.-P. Yan, *J. Phys. Chem. C* **2009**, *114*, 311 – 316.
[23] Y. Zhou, W. Zhou, *CrystEngComm* **2012**, *14*, 1449 – 1454.
[24] a) S. I. Abu-Eishah, A. M. Dowaidar, *J. Chem. Eng. Data* **2008**, *53*, 1708 – 1712; b) F. Suzuki, K. Onozato, N. Takahashi, *J. Appl. Polym. Sci.* **1982**, *27*, 2179 – 2188.

